Popular Summary:

"Reducing the Uncertainties in Direct Aerosol Radiative Forcing"

R.A. Kahn, 2011.

Surveys in Geophysics, in press.

Airborne particles, which include desert and soil dust, wildfire smoke, sea salt, volcanic ash, black carbon, natural and anthropogenic sulfate, nitrate, and organic aerosol, affect Earth's climate, in part by reflecting and absorbing sunlight. This paper reviews current status, and evaluates future prospects for reducing the uncertainty aerosols contribute to the energy budget of Earth, which at present represents a leading factor limiting the quality of climate predictions. Information from satellites is critical for this work, because they provide frequent, global coverage of the diverse and variable atmospheric aerosol load.

Both aerosol amount and type must be determined. Satellites are very close to measuring aerosol amount at the level-of-accuracy needed, but aerosol type, especially how bright the airborne particles are, cannot be constrained adequately by current techniques. However, satellite instruments can map out aerosol air mass type, which is a qualitative classification rather than a quantitative measurement, and targeted suborbital measurements can provide the required particle property detail. So combining satellite and suborbital measurements, and then using this combination to constrain climate models, will produce a major advance in climate prediction.

Reducing the Uncertainties in Direct Aerosol Radiative Forcing

Ralph A. Kahn

Abstract Direct aerosol radiative forcing (DARF) remains a leading contributor to climate prediction uncertainty. To monitor the spatially and temporally varying global atmospheric aerosol load, satellite remote sensing is required. Despite major advances in observing aerosol amount, type, and distribution from space, satellite data alone cannot provide enough quantitative detail, especially about aerosol microphysical properties, to effect the required improvement in estimates of DARF and the anthropogenic component of DARF. However, the combination of space-based and targeted suborbital measurements, when used to constrain climate models, represents an achievable next step likely to provide the needed advancement.

1 Introduction

Airborne particles, which include desert and soil dust, wildfire smoke, sea salt, volcanic ash, black carbon, natural and anthropogenic sulfate, nitrate, and organic aerosol, affect Earth's energy budget both directly, by reflecting and absorbing sunlight, and indirectly, by altering cloud microphysical processes. This paper reviews the current status, and evaluates future prospects for quantifying a major component of the aerosol influence on Earth's climate system, through the direct radiative impact on incoming solar radiation. Aerosol-cloud interactions, and the indirect aerosol radiative effects that these produce, are beyond the scope of the current paper. Global-scale observational constraints on the indirect processes are much less well established and, as such, the continuum between "clear-sky" conditions, which are the subject of this paper, and "all-sky" conditions (e.g., Várnai and Marshak 2011), is considered here only in the context of the cloud masking techniques applied to aerosol remote-sensing observations.

R. A. Kahn (✉)
Laboratory for Atmospheres, NASA Goddard Space Flight Center, Greenbelt, MD 20771, USA
e-mail: ralph.kahn@nasa.gov

Springer

The Intergovernmental Panel on Climate Change (IPCC) assessment of direct aerosol radiative forcing (DARF) uncertainty changed from "Very Low" to "Medium–Low" between their Third Assessment Report (IPCC 2001), completed as data from NASA's earth observing system (EOS) satellites were just becoming available, and their Fourth Assessment 6 years later. The IPCC uncertainties are estimated in light of the diversity in performance among a collection of benchmark climate models. Their DARF uncertainty designations represent the first and third rungs, respectively, of a five-step scale that reports consensus judgment, based upon available physical and chemical evidence. Between the third and fourth IPCC assessment reports, a climatology of global, monthly aerosol optical depth (AOD) was produced by combining data from the EOS Multi-angle imaging spectro-radiometer (MISR) and MODerate resolution imaging spectro-radiometer (MODIS) instruments, with ground-based values obtained from the Aerosol Robotic Network (AERONET; Kinne et al. 2006). The resulting AOD constraints made a key contribution toward reducing the reported model uncertainty (Haywood and Schulz 2007).

However, DARF uncertainty remains a limiting factor for reducing global average radiative forcing assessment, as the model-based estimated value is about -0.5 ± 0.4 Wm^{-2} (i.e., net cooling) for the global anthropogenic, all-sky, top-of-atmosphere component, assessed since the pre-industrial era (IPCC 2007), and is about $-1.1 \pm 0.4\ Wm^{-2}$ for clear-sky conditions over ocean (CCSP 2009); for comparison, the CO_2 forcing is given as $1.66 \pm 0.17\ Wm^{-2}$ (IPCC 2007). Calculations suggest that instantaneous, mid-visible AOD measurement accuracy of about 0.02 is typically required under cloud-free conditions to constrain DARF to approximately $1\ Wm^{-2}$ (McComiskey et al. 2008; CCSP 2009), whereas the corresponding uncertainties in the current global AOD products from MISR and MODIS are 0.03 or larger over dark water, and 0.05 or larger over land (Kahn et al. 2010; Levy et al. 2010; Remer et al. 2005). Theoretical DARF sensitivity analysis identified particle single-scattering albedo (SSA) as the other leading factor in most situations, especially important for determining radiative forcing over land surfaces, and requiring an instantaneous constraint of about 0.02, though varying with other factors, particularly AOD and surface albedo (McComiskey et al. 2008).

Perturbation studies based on one-dimensional radiative transfer calculations suggest that the quantitative uncertainties reported by the IPCC (2007), which were derived only from model diversity rather than aggregated error, are actually underestimated by a factor between two and four (Loeb and Su 2010). This study also concludes that, along with AOD, SSA uncertainty makes a leading contribution to overall DARF uncertainty, especially when clouds are present. A separate assessment of DARF uncertainty was performed by comparing forward simulations of DARF over the industrial era, with the same quantity calculated from the difference between (1) overall climate model forcing required to reproduce the temperature record, and (2) all forcing elements other than aerosol (Anderson et al. 2003). For the anthropogenic aerosol component, the differences between these two estimates were significant: the estimate was approximately $-1.0\ Wm^{-2}$ for the inverse calculations, and a statistically larger net cooling of roughly $-1.5\ Wm^{-2}$ for the forward approach, with scatter of order $\pm 0.5\ Wm^{-2}$ for both methods.

One consequence of the current DARF uncertainty is the limitation it places on constraining climate model predictive ability (Anderson et al. 2003, 2005; Kiehl 2007; Schwartz et al. 2010). In its simplest form, a model's climate sensitivity, λ $(K/(Wm^{-2}))$ is often represented as a factor linearly relating the model-predicted change in global-mean surface temperature (GMST), ΔT, to an increase in effective global-mean forcing, ΔF:

$$\Delta F = \lambda^{-1} \Delta T + N \tag{1}$$

Here, N is the global heat content rate-of-change, associated primarily with warming of the ocean, that approaches zero as equilibrium relative to a perturbed forcing is reached. The climate sensitivity term includes the modeled climate feedbacks; complicating factors include the time-scale over which the forcing acts, and that required for the system to relax to equilibrium, as well as the need to account for regional differences in assessing the global aggregate, nonlinear aspects of the system, and whether total or only anthropogenic aerosols are considered. (Note that, although DARF typically refers to direct radiative forcing by all aerosols, the term "Direct Aerosol Climate Forcing" is sometimes used to mean the direct forcing due to anthropogenic aerosols alone. To avoid confusion, the term "anthropogenic component of DARF" is used here, when that is intended.)

A key method of evaluating climate model performance overall is to compare the simulated global mean surface temperature (GMST) during the twentieth century with the observed temperature record for the same period, when the model forcing includes best-estimate greenhouse gas accumulation, solar variability, and aerosol effects, so uncertainty in DARF translates directly into model climate sensitivity uncertainty. As such, DARF is a leading factor limiting the confidence with which current climate models can predict changes in GMST (IPCC 2007), and among 11 widely cited climate models that reproduce the twentieth-century temperature anomaly, climate sensitivity is inversely related to the assumed anthropogenic forcing, of which aerosol forcing contributes the largest uncertainty (Kiehl 2007). The IPCC (2007) best estimate for λ is 0.8 K/(Wm^{-2}), with a one-σ range of about 0.54–1.2 K/(Wm^{-2}) based again on model diversity, so loosely translating DARF uncertainty into modeled equilibrium GMST uncertainty, DARF uncertainty of 1 Wm^{-2} yields a best-estimate GMST uncertainty of 0.8 K, ranging to values in excess of 1 K.

This paper provides a brief review the strengths and limitations of aerosol measurements that bear upon current, short-wave DARF under cloud-free conditions, and discusses how the contributions of satellite and suborbital measurements, when combined with aerosol transport modeling, can reduce the uncertainties in DARF.

2 What Satellites Offer

Aerosols are especially challenging to study because they originate from many, diverse sources, both natural and anthropogenic, and exhibit an enormous range of chemical compositions and physical properties. Unlike long-lived atmospheric gases, airborne particles are typically removed from the troposphere by precipitation or gravitational settling within about a week, so aerosol amount and type vary dramatically on many spatial and temporal scales. For this reason, the frequent, global coverage provided by space-based remote-sensing instruments has played a central role in the study of aerosol impacts on the global energy budget (e.g., Bellouin et al. 2008; Kim and Ramanathan 2008; Loeb and Manalo-Smith 2005; Myhre et al. 2009; Quaas et al. 2008: Yu et al. 2006).

This section gives an overview of passive aerosol remote-sensing capabilities from space; in addition to the references cited below, further detail about many of the retrieval algorithms involved can be found in Kokhanovsky et al. (2009) and de Leeuw et al. (2011).

2.1 Early Aerosol Optical Depth (AOD) Measurements

The aerosol parameter most commonly derived from spacecraft remote-sensing data, and used in global energy budget calculations, is total-column, mid-visible, aerosol extinction

optical depth. It is a measure of aerosol amount based on the fraction of incident light that is either scattered or absorbed by particles, integrated over the vertical column through the depth of the atmosphere. Formally, AOD is a dimensionless quantity, the product of the particle number concentration, the particle-effective extinction cross-section (which accounts for particle scattering + absorption), and the path length through the atmosphere, assessed along an effective vertical path.

To infer AOD from the upwelling radiances observed by space-based passive imagers, retrieval algorithms must sort out surface from atmospheric contributions, must account for particle absorption and the angular variation of particle light-scattering intensity, as well as scene heterogeneity, cloud contamination, and any gaseous absorption in the spectral bands used. The problem is underdetermined, and assumptions are made, as needed, depending on the retrieval approach adopted. Most retrieval algorithms to date assume the aerosol is horizontally homogeneous over the retrieval region, which can be comprised of one or more pixels. Different approaches are often applied depending on surface type; it is generally easier to perform aerosol retrievals with these data over dark, uniform ocean or dark land than brighter surfaces or terrain that is topographically complex or variable on retrieval-region length scales. Much creative effort during the past 30 years has focused on developing reliable overland remote-sensing retrieval methods. Aerosol vertical distribution is usually either assumed or adopted from external models or measurements (e.g., Sect. 2.4 below). The required particle optical properties are either assumed based on climatological considerations, or constrained as part of self-consistent interpretation of the observed radiances.

The advanced very high resolution radiometer (AVHRR) imagers have been collecting daily, global, multispectral data from polar orbit since late 1978 (Table 1). Although these instruments were designed primarily to observe Earth's surface, over-ocean, total-column AOD has been derived, initially from single-channel observations, assuming a completely dark ocean surface in the red band (0.63 micrometers effective wavelength) along with medium-sized, purely scattering particles (Stowe et al. 1997). Subsequently, two-channel retrievals were performed (Mishchenko et al. 1999; Ignatov et al. 2004), adding the 0.85 micrometer band, refining the assumed ocean surface reflectance model, and also retrieving the Ångström exponent (ANG, related to the spectral slope of AOD), a quantity that can provide some indication of particle size. Similarly, AOD retrieval algorithms have been developed for imagers aboard geostationary satellites, such as NOAA's GOES series (Knapp 2002) and European Space Agency's Spinning Enhanced Visible and Infrared Imager (SEVIRI; Popp et al. 2007; Wagner et al. 2010), providing high-temporal-resolution products as frequently as every 15 or 30 min, making it possible to at least qualitatively map the development of aerosol plumes. Although broad spectral bands and poor radiometric calibration limit the quantitative application of these data, early results demonstrated the long-range, over-ocean transport of dust, smoke, and pollution particles from terrestrial sources (e.g., Husar et al. 1997), highlighting the need to consider aerosol effects on the global energy budget.

Other remote sensing approaches are required to separate the surface from atmospheric contributions to the observed scene brightness, making it possible to retrieve AOD over more reflective coastal regions and most land. Due to the intense scattering of ultraviolet (UV) light by atmospheric molecules, the surface is obscured when viewed from space in the wavelength range 0.33–0.38 micrometers, and many types of surfaces themselves are relatively dark in the UV. In the late 1990s, it was realized that the total ozone mapping spectrometers (TOMS), versions of which had already been orbiting for nearly 20 years, contained the spectral channels needed to detect aerosols over land as well as water, based

Table 1 Major, currently available, satellite tropospheric aerosol data products

Sensor/platform	Spatial coverage	Temporal coverage	Retrieved aerosol parameters	Leading sources of AOD uncertainty
AVHRR/NOAA-series	~Daily, global ocean	1981–present	AOD, ANG	CAL, CLD, TYP
TOMS/Nimbus, ADEOS1, EP	~Daily global, land & ocean	1979–2001	AOD, AAI, SSA, AAOD	HT, CLD, CAL, TYP, RES
ATSR-2/ERS-2; Advanced-ATSR/ENVISAT	~Weekly global, land & ocean	1995–2003; 2003–present	AOD, ANG	TYP, CLD, CAL
GOME/ERS-2; GOME-2/METOP	~Weekly global, land & ocean; ~daily global, land & ocean	1995–2003; 2007–present	AAI, AOD, TYP in synergy with ATSR-2/AVHRR	RES, SURF, HT, CLD, CAL
POLDER-1, -2, PARASOL	~Daily global, land & ocean	1997–present	AOD, ANG, NSPH (fine-mode over land)	CAL, CLD, TYP
MODIS/Terra, Aqua	~Daily global, land & ocean	2000–present (Terra) 2002–present (Aqua)	AOD, ANG (ocean), FMF (ocean)	CAL, CLD, TYP, SURF (over land)
MISR/Terra	~Weekly global, land & ocean + bright desert & nadir sun-glint	2000–present	AOD, ANG, SML, NSPH, SSA (2–4 bins), PH	CLD, CAL, TYP
GLAS/ICESat	Global curtain, land & ocean, 16-day repeat cycle	2002–present (~3 months/year)	Extinction/backscatter VP	–
SEVIRI/MSG	15 min intervals, Europe, Africa, Atlantic	2003–present	AOD	CAL, TYP, SURF
SCIAMACHY/ENVISAT	~Weekly global, land & ocean	2003–present	AAI; AOD, TYP in synergy with ATSR	CAL, SURF, CLD, TYP
MERIS/ENVISAT	~3-day global, land & ocean	2003–present	AOD	CLD, TYP, SURF
OMI/Aura	~Daily global, land & ocean	2004–present	AOD, AAI, SSA, AAOD	HT, CLD, CAL, TYP
CALIOP/CALIPSO	Global curtain, land & ocean, 16-day repeat cycle	2006–present	VP: extinction/backscatter, color ratio, depolarization ratio, AOD	EBR, CAL, CLD, D_SNR

Sources of uncertainty vary with conditions; they are listed in approximate order of significance

AOD aerosol optical depth, *AI* aerosol index, *ANG* Ångström exponent, *TYP* aerosol type, *AAI* absorbing aerosol index, *FMF* fine-mode fraction, *SML* AOD fraction small, medium, large, *SSA* single-scattering albedo, *AAOD* absorbing AOD, *NSPH* fraction AOD nonspherical, *PH* near-source plume height, *VP* vertical profile, *CAL* radiometric calibration, *CLD* cloud contamination, *TYP* aerosol-type assumption or constraint, *HT* aerosol layer height, *SURF* bright surface reflectance, *RES* spatial resolution, *EBR* extinction/backscatter ratio (a function of aerosol type), *D_SNR* signal/noise ratio for daytime observations (e.g., Kacenelenbogen et al. 2011)

on aerosol absorption of the upwelling background UV light (Herman et al. 1997). This resulted in the Aerosol Index or Absorbing Aerosol Index, a qualitative measure of UV-absorbing aerosols such as dust and smoke, subsequently converted to quantitative estimates of AOD using a combination of available constraints and assumptions about aerosol type (Torres et al. 1998). A similar approach has been used to derive Aerosol Index from the GOME series of satellites, over coarse surface sampling regions averaging about 40×320 km (de Graaf et al. 2005). These retrievals have limited sensitivity to near-surface aerosols, and depend sensitively on the altitude of the particles and their optical properties, but the TOMS maps provided the first comprehensive, long-term record of aerosol source regions and overland transports (e.g., Torres et al. 2002; Prospero et al. 2002). A next-generation ozone monitoring instrument (OMI), with additional spectral channels in the visible, and 13×24 km sampling resolution at nadir (compared to 39×39 km for the Earth Probe TOMS, the latest in the series), has been flying aboard the EOS Aura spacecraft since July 2004. AOD at UV and visible wavelengths, as well as estimates of column-effective SSA, are routinely derived from OMI observations (Torres et al. 2007).

One of the first and most widely used aerosol remote-sensing techniques is surface-based sun photometry, a multi-angle approach that involves measuring the instantaneous intensity of the solar disk in narrow (~ 10 nm wide) bands in spectral regions of minimal gaseous absorption. The method predates satellite observations (e.g., Flowers et al. (1969), who present the results of a remarkable network of about 40 Voltz sun photometers across the United States), and relies on highly accurate radiometric calibration. Calibration is achieved for reference instruments by the Langley method: the systematic increase in atmospheric opacity and the corresponding decrease in solar brightness, are observed as the sun is viewed through longer atmospheric slant paths at stable, pristine mountain top observatories. Subsequently, field instruments are inter-calibrated with these references. AOD is measured, typically at multiple wavelengths, allowing some information about particle size to be derived. Though they offer only limited spatial coverage, networks of autonomous surface-based sun photometers have been deployed, such as AERONET (Holben et al. 1998), a global federation of several hundred stations, and SkyNet in East Asia (Kim et al. 2004); ships-of-opportunity provide additional AOD validation measurements in the generally under-sampled ocean regions (Smirnov et al. 2009). When pre- and post-observation instrument calibration is performed, the measured mid-visible AOD accuracy is estimated at about 0.01 for the AERONET CIMEL instruments (Eck et al. 1999); the results are used in part to validate the assumptions needed to retrieve AOD and ANG from space, by both statistical and event-by-event comparisons with the satellite retrievals (e.g., Remer et al. 2005; Levy et al. 2010; Kahn et al. 2010).

Multi-angle approaches have also been applied to space-based observations, beginning in 1995 with the European Space Agency (ESA) two-view-angle Along-Track Scanning Radiometer-2 (ATSR-2) imager (Veefkind et al. 1998, 2000; North 2002; Table 1). The satellite technique measures light scattered by the scene below, so unlike the situation for surface-based sun photometry, additional assumptions about aerosol and surface optical properties are required to retrieve column-integrated AOD. However, the atmospheric contribution to the signal, relative to that of the surface, increases systematically as the slant path increases, making surface-atmosphere separation possible. The steeper slant paths also improve sensitivity to thinner aerosol layers.

A third approach, in addition to UV and multi-angle, for separating surface from atmospheric signals in top-of-atmosphere observations was pioneered by the French Space Agency (CNES), which began flying their POLarization and Directionality of the Earth's

Reflectances (POLDER) series of imagers in 1996 (Deschamps et al. 1994). The POLDER instruments collected multi-angle, multispectral polarization data from orbit, at a pixel resolution of about 6 km at the sub-spacecraft point. Over most common land surface types, except bright desert, the polarization effects are fairly independent of wavelength (Waquet et al. 2009), making it possible to separate the more constant surface polarization contribution to the satellite signal from the spectrally varying atmospheric contribution.

Aerosols are sometimes divided into two size groups, depending on whether their effective diameter is greater or less than a certain size, usually taken to be around 1 micrometer for satellite and some field observations, and 2.5 micrometers for air quality applications. These distinctions are somewhat arbitrary, but are based on loose physical considerations (e.g., Whitby 1978); the majority of smoke and aerosol pollution particles, the products of combustion and chemical processing, tend to fall into the smaller "accu-mulation" or "fine" mode. Mechanically produced desert dust and sea salt particles tend to be weighted toward the "coarse" mode. And, if inhaled, particles smaller than about 2.5 micrometers in diameter are more likely to penetrate the lungs. From its combination of optical measurements, POLDER maps column-integrated fine-mode and total aerosol optical depth over water, as well as fine-mode optical depth over land (Deuzé et al. 2001; Herman et al. 2005).

2.2 AOD Measurements in the EOS Era

The MISR and MODIS instruments were launched into a sun-synchronous polar orbit with a 10:30 local equator-crossing time, descending on the dayside, in December 1999 aboard the EOS Terra satellite (Table 1). They were designed with enhanced capabilities for monitoring aerosols from space, compared to earlier efforts. A second MODIS instrument was deployed aboard the EOS Aqua satellite in May 2002, in a polar orbit having a 1:30 local equator-crossing time, ascending on the day side. MODIS follows the multispectral approach of the AVHRR instruments, but with higher spatial resolution (a maximum of 250 m, compared with 1 km for AVHRR), 36 spectral channels, and much higher radio-metric calibration accuracy and stability. Global, total-column AOD over cloud- and glint-free ocean, as well as darker land surfaces, is produced routinely every 2 days, along with fine-mode fraction over ocean (Kaufman et al. 1997; Tanré et al. 1997; Remer et al. 2005; 2008; Levy et al. 2010).

Over ocean, standard glint and whitecap models are applied, and the surface is assumed dark at red and near-infrared wavelengths; using a look-up table approach, the algorithm selects the best-matching simulated radiances derived from assumed combinations of one fine-mode and one coarse-mode component (Remer et al. 2005). Several new techniques were developed to separate surface from atmospheric signals for multispectral, single-view imagers observing over land. For example, the top-of-atmosphere radiance in the MODIS 2.1 micrometer channel, for which the aerosol and atmospheric gas opacities (except water vapor in some places) are much lower than in the visible bands, with AOD often negligible, is used to determine the surface reflectance at this wavelength. The 2.1 micrometer reflectance is then used to evaluate the 0.47 and 0.67 micrometer surface reflectances, based on empirically derived relationships that depend on viewing geometry and a surface greenness index (Kaufman et al. 1997; Levy et al. 2007). Lacking sensitivity to particle type over land, the MODIS algorithm assumes particle types based on a climatology derived from AERONET observations (Levy et al. 2007). A similar approach is planned for the next-generation of U.S. geostationary satellites (Laszlo et al. 2008).

A related method has also been applied to data from the medium resolution imaging spectrometer (MERIS) aboard ESA's polar-orbiting ENVISAT spacecraft. However, the 15 programmable MERIS spectral bands do not extend as far into the near-infrared as those of MODIS, so a vegetation index calculated from 0.675 and 0.870 micrometer radiances is used to constrain the surface reflectance (von Hoyningen-Huene et al. 2007).

Yet another technique for retrieving AOD over land is based on looking at the time-dependent variation in measured radiance. By carefully selecting dark pixels in a time-series of images, representing the surface reflectance under cloud-free conditions and having the lowest available AOD, the AOD on hazier days can be estimated; this method has been applied to aggregates of geostationary satellite data about 2 weeks in length, taken at the same time-of-day to assure similar solar geometry (Knapp et al. 2007). For MODIS, up to 16 days of observations, capturing a range of view angles and atmospheric conditions, have been used in an automated algorithm to determine the 2.1–0.47 micrometer surface reflectance ratio dynamically, and to retrieve column-effective AOD, ANG, and surface bidirectional reflectance properties simultaneously at 1 km resolution (Lyapustin and Wang 2009; Lyapustin et al. 2011). Efforts are also being made, using the 0.412 micrometer "deep blue" channel, to extend the MODIS aerosol retrieval over land surfaces such as desert that are relatively dark in this band, but brighter at longer wavelengths (Hsu et al. 2004, 2006). In addition, MODIS thermal infrared channels are used to detect thermal hot spots, which can help locate fires and identify the associated smoke plumes (Giglio et al. 2006; Ichoku et al. 2008).

MISR complements MODIS, acquiring four-spectral-channel, near-simultaneous views of Earth at nine angles, spatial sampling up to 275 m/pixel, and similarly high radiometric calibration accuracy ($\sim$3% absolute, 1.5% band-to-band) and stability (Diner et al. 1998). Having a narrower swath than MODIS, MISR takes about a week to image the entire planet. With the multi-angle coverage, AOD and surface reflectance are retrieved self-consistently over land, including bright desert surfaces, providing more accurate AOD overland results, compared to other techniques (Martonchik et al. 2002, 2009). The nine views also sample light scattered in different directions, which yields some information about column-averaged particle size, shape, and SSA under favorable retrieval conditions (Kahn et al. 2010; Sect. 2.3 below).

For aerosol retrievals aimed at clear-sky conditions, cloud screening is an essential component of the algorithms. Brightness thresholds are routinely used, in the thermal infrared, when available, to identify cold, high clouds, and in the visible and near-infrared, for clouds having sufficient optical depth at these wavelengths (e.g., Ackerman et al. 1998; Remer et al. 2005; Stowe et al. 1998; Zhao and Di Girolamo 2004). Scene variability at high spatial resolution is applied in the MODIS algorithm over water to identify heterogeneity likely to be due to cloud (Martins et al. 2002), and the MODIS 1.38 micrometer channel is used to provide greater sensitivity to high, thin cirrus in the aerosol algorithm (Gao et al. 2002). For MISR, the angular information is applied in several ways, including changes in the reflected-light spectral ratio with angle (Di Girolamo and Wilson 2003) and stereo-derived heights (Moroney et al. 2002) to identify reflecting layers above the nominal surface, as well as angular smoothness and angle-to-angle spatial correlation tests to detect cloud edges, changes in the scene during multi-angle data acquisition, and sub-pixel scene heterogeneity (Martonchik et al. 2002, 2009).

However, these cloud-screening techniques sometimes mask thick aerosol plumes and, more generally, they offer limited sensitivity to clouds having visible optical depth below a few tenths. Systematic increases in MODIS-retrieved AOD with cloud fraction are observed (e.g., Loeb and Manalo-Smith 2005; Zhang and Reid 2006), and effects including

aerosol humidification near clouds (Twohy et al. 2009; Tackett and Di Girolamo 2009), sub-pixel cloud contamination (Zhao et al. 2009), and the three-dimensional effects of cloud-scattered light (Marshak et al. 2008), have been identified as likely contributors under different conditions. Efforts at quantifying the contribution of clouds to the MODIS AOD identified a net bias of about 0.02 (Kaufman et al. 2005a), but the transition regions between cloudy and cloud-free atmosphere are not well resolved in the satellite observations, and validation data are scarce, so considerable uncertainty remains in this aspect of retrieval quality.

To evaluate confidence over the entire range of retrieved AOD values, an absolute criterion is needed to take account of the lower limit of AOD measurement sensitivity (e.g., 0.03 or 0.05), and in addition, a relative criterion (e.g., percent of AOD) is required to adequately represent AOD variability and other factors that scale as AOD itself (Kahn et al. 2011). Based on statistical comparisons with large numbers of near-coincident AERONET surface sun photometer observations, the Collection 5 MODIS AOD product confidence envelope (1σ) is $\pm(0.03 + 5\%$ of AOD) over dark water (Remer et al. 2005), and $\pm (0.05 + 15\%$ of AOD) over land (Levy et al. 2010). The Version 22 MISR overall confidence envelope, assessed more conservatively than the MODIS studies, amounts to the larger of 0.05 or 20% of AOD, with higher confidence over water (Kahn et al. 2010).

These AOD assessments do have limitations. For example, there are significant gaps in the global distribution of sun photometer sites, and apparent AOD discrepancies are often caused by actual AOD variability on kilometer scales, as sampled differently by the satellite vs. the ground-based instruments. And these comparisons can be made only when the satellite and surface instrument cloud masks both report cloud-free conditions; this precludes evaluating the satellite cloud-masking methods with these data.

Nevertheless, the validation results show that although the required instantaneous AOD accuracy of about 0.02 has not yet been achieved, it is within reach. The contribution already made by the combined MISR, MODIS, and AERONET data toward constraining climate model AOD and the resulting DARF estimates was discussed in Sect. 1. The same data combination has also made it possible to identify regional, and to some extent global, over-ocean AOD trends for the decade beginning in 2000 (Zhang and Reid 2010). Efforts to extend the record back through the early years of AVHRR have met with success in documenting regional trends over ocean, providing results consistent with regional patterns of observed solar dimming (Mishchenko and Geogdzhayev 2007), but the advances offered by the EOS-generation instruments are apparently required to isolate global-average behavior over ocean (Zhang and Reid 2010). AOD trends are especially difficult to assess, in part because they represent only one possible component of AOD variability, and individual outlier events can sometimes confuse a simple trend analysis (see, e.g., Kahn et al. 2011). As longer time-series become available, the analysis of AOD trends over ocean will become more tractable, though the greater challenge of identifying and quantifying trends over land awaits additional retrieval algorithm refinement and/or new instrumentation.

Improvements to the present MISR and MODIS AOD products rest in part on reducing radiometric calibration uncertainties, but primarily on upgrading the assumptions used to help constrain aerosol type, that are an essential component of the AOD retrieval process (Kahn et al. 2010; Levy et al. 2010). The assumed aerosol vertical distribution and surface reflectance must also be considered when interpreting observed top-of-atmosphere radiance signals in terms of AOD. We turn to these factors in the next two subsections.

2.3 Aerosol Type

The spectral dependence of AOD contains some information about particle size (King et al. 1978), and this is the basis for reporting ANG and fine-mode-fraction in the AVHRR and MODIS over-ocean products. Desert dust and sea salt tend to have higher fractions of coarse-mode particles, whereas smoke, secondary organic aerosol, and pollution particles tend to be fine-mode dominated. One caveat with this aerosol-type identification approach is that interpretation of ANG is ambiguous, especially when multiple aerosol modes are present in the atmospheric column (Schuster et al. 2006), which is a common occurrence. Yet, the fine-to-coarse AOD ratio from these instruments exhibits the generally expected regional and seasonal patterns, especially for desert dust from the Sahara and smoke originating from sub-Saharan grassland or tropical forest fires that is subsequently advected over the Atlantic, lending confidence to the results (Mishchenko et al. 1999; Remer et al. 2008).

Kaufman et al. (2005b) took the further step of interpreting the combination of MODIS over-ocean AOD and fine-mode fraction in terms of "anthropogenic" AOD. To accomplish this, they assume that a fixed fraction of fine-mode aerosol is smoke from natural sources, and that the tails of the dust and sea spray size distributions contribute fixed fractions to the fine-mode AOD, based on observations under relatively well-constrained conditions. This approach again reproduces generally expected patterns, but the results are easily over-interpreted, as the information content of the MODIS data is limited to a qualitative size constraint, and the actual size-resolved fractional contributions of different aerosol components vary immensely with conditions.

By combining the column AOD from MODIS with collocated UV radiances from OMI under cloud-free conditions, ambiguities in the OMI retrieval associated with aerosol altitude, total aerosol amount, and sub-pixel cloud contamination can be reduced, so tighter constraints on both aerosol layer height and UV absorption can be obtained than is possible from OMI alone (Satheesh et al. 2009). A paucity of coincident ground-truth data precludes quantitative validation of the retrieved UV SSA, but the relative values give an indication of the regionally and seasonally varying dust and smoke distributions.

Multi-angle views and polarized channels yield additional constraints on particle type. For example, the polarized multi-angle, multispectral radiance measurements from POL-DER contain information on particle shape as well as size. Depolarizing desert dust can be distinguished from spherical particle types (Deuzé et al. (2001), and over ocean, fine- and coarse-mode AOD values can be derived, along with the coarse-mode nonspherical component AOD (Herman et al. 2005).

A classification of aerosol type, based on column-averaged particle size, shape, and SSA constraints, can be derived from the MISR multi-angle, multispectral observations (Fig. 1). The instrument can distinguish about three-to-five groupings based on particle size, two-to-four groupings in SSA, and spherical vs. nonspherical dust and cirrus particles (Chen et al. 2008; Kahn et al. 2001, 2010; Kalashnikova and Kahn 2006; Pierce et al. 2010). Although AOD retrievals tend to be robust under different scene conditions due to the systematic variation in atmospheric slant path observed by the MISR cameras, aerosol-type information varies considerably with the range of scattering angles sampled, with surface reflectance properties, and with AOD itself. As such, MISR aerosol-type information is essentially categorical, making it possible to map out about a dozen aerosol air-mass types globally when the AOD is greater than about 0.15, observations at an adequate range of scattering angles are obtained, and the surface is sufficiently uniform or well defined
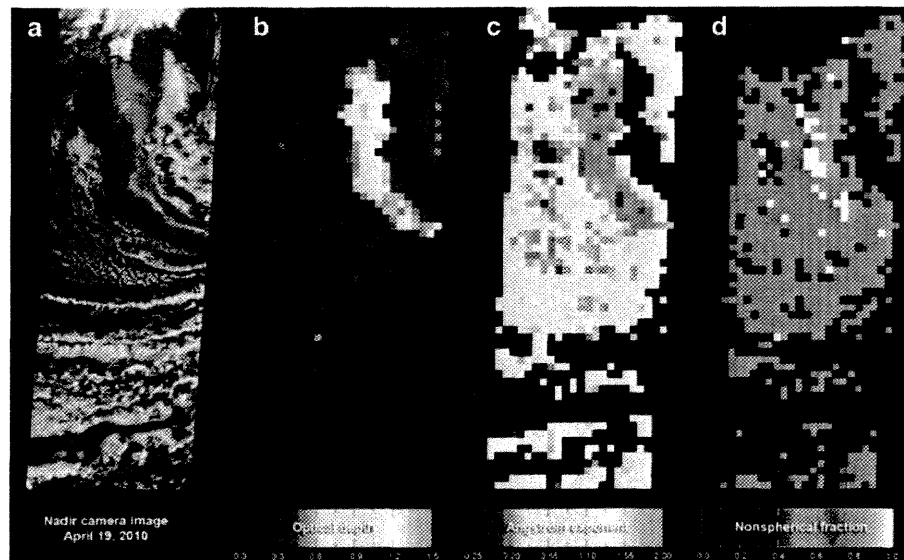
Fig. 1 An example of aerosol amount and type mapping from MISR. **a** This true-color, nadir view shows the (*brown*) ash plume emanating from Iceland's *Eyjafjalljökull* volcano, at about 12:51 UTC on April, 19 2010. The volcano itself is at the top-center of the image. The plume stands out as having higher mid-visible AOD (**b**) and being dominated by larger particles (lower ANG, **c**), than the background. The ash plume appears, but is less distinct, in the fraction AOD nonspherical map (**d**), as the algorithm also picks up some adjacent nonspherical cirrus. The aerosol properties are reported on 17.6 km retrieval regions. Ash from several eruptions of this volcano during Spring 2010 curtailed air traffic over much of Europe [*MISR Team, Jet Propulsion Lab/Caltech and NASA Goddard Space Flight Center*]

(Kahn et al. 2010). However, this information alone is not enough to provide the detailed particle microphysical properties required to fully constrain DARF.

A multispectral method has also been applied to synergetically exploit data from two instruments aboard ESA's ENVISAT spacecraft: the 1 km pixel-resolution AATSR radiometer for cloud screening and AOD retrieval, and the SCanning Imaging Absorption spectroMeter for Atmospheric CHartographY (SCIAMACHY) spectrometer to constrain aerosol type. Only the nadir view is used for the aerosol-type classification, which relies upon fitting spectral reflectances at 10 visible wavelengths from 405 to 670 nm; with the coarse SCIAMACHY spatial resolution of at about $30 \times 60 \text{ km}^2$, four broad aerosol categories, water-soluble, soot, mineral dust, and sea salt, can be differentiated (Holzer-Popp et al. 2008).

Aerosol type has also been retrieved from active sensor data. Specifically, a layer-resolved aerosol-type classification has been produced from the combination of spectral backscatter, extinction, and polarization measurements made by the lidar aboard the Cloud-Aerosol Lidar and Infrared Pathfinder Satellite Observations (CALIPSO) spacecraft, flying since 2006 in formation with the EOS Aqua satellite carrying MODIS (Cattrall et al. 2005). Based on a clustering of optical properties measured by the active lidar sensor, qualitative distinctions among typical maritime, desert dust, biomass burning, and urban/industrial particles can be made, along with a mixture of types common in SE Asia.

One factor, in addition to the information content of the satellite remote-sensing data, limiting the quantitative assessment of aerosol type from spacecraft is a lack of validation

data. By scanning across the almucantar in addition to making direct-sun measurements, the AERONET surface stations collect the data needed to retrieve several modes of column-integrated particle size distribution, along with constraints on column-effective (though not component-specific) SSA and particle sphericity (Dubovik and King 2000; Dubovik et al. 2006). Despite limited sampling, and significantly more assumptions than are required for the direct-sun spectral AOD measurements, these observations represent among the most extensive aerosol-type data available, and they have been used to derive general-purpose aerosol-type climatologies (Dubovik et al. 2002; Eck et al. 2008, 2010). AERONET-based climatologies have also been developed specifically for use in the CALIPSO (Omar et al. 2009) and the MODIS overland (Levy et al. 2007) retrievals.

In addition to sampling issues, the surface-based sun-sky radiometer constraints on SSA require AOD $> \sim 0.4$ at 0.44 micrometers, a criterion achieved infrequently in many parts of the world, though not in some regions dominated by major anthropogenic emissions, including major urban areas of North America and Europe, and parts of China and India. And AERONET-retrieved column-effective SSA does not distinguish between different aerosol modes or layers in the atmosphere. However, species-specific aerosol chemical and microphysical property validation data can be obtained with much greater detail from surface and aircraft direct sampling. Such measurements can provide the most accurate size distribution, SSA values, and chemical composition currently available, but sampling is extremely limited; coincident aircraft and satellite observations, obtained on field-campaign "Golden Days," can critically test aerosol-type retrievals, but only on these very special occasions (e.g., Kahn et al. 2009).

In summary, qualitative aerosol-type classifications have been produced from both passive and active EOS-era remote sensors, yielding broad-swath, column-effective, and layer-resolved curtain coverage, respectively. This represents a major advance in capability but, in itself, does not provide sufficient microphysical detail to resolve DARF uncertainties, nor does it provide the compositional constraints required to identify the anthropogenic aerosol component.

2.4 Aerosol Vertical Distribution and Surface Reflectance

Aerosol vertical distribution is a contributing factor when calculating DARF, especially for absorbing species, and it is also of primary importance for assessing aerosol transports and material fluxes (e.g., Yu et al. 2008). The highest-accuracy space-based measurements of aerosol vertical distribution are obtained from lidar, which can detect multiple aerosol layers day and night, as optically thin as 0.005 at mid-visible wavelengths, though signal-to-noise is lower under daylight conditions (Winker et al. 2009). Space-based lidar makes it possible to create a global, climatological picture of transported aerosols, but the lidar swath is the width of the laser beam, about 70 meters in size for CALIPSO, so coverage of specific sites or events is serendipitous (e.g., Kahn et al. 2008). The technique was demonstrated in 1994, with the Lidar In-space Technology Experiment (LITE) aboard NASA's Space Shuttle Discovery, and has been followed by the geoscience laser altimeter system (GLAS) and CALIPSO instruments on polar-orbiting EOS satellites (Table 1). The vertical resolution of the CALIPSO observations is as high as 30 m, and the horizontal resolution of the CALIPSO profile product is as high as 330 m, though it can be reduced when greater horizontal spatial averaging is applied to enhance signal-to-noise (Winker et al. 2009).

As discussed in Sect. 2.3 above, the TOMS/OMI passive aerosol retrieval technique is sensitive to layer height for UV-absorbing aerosols, and by combining these data with a constraint on total-column AOD, elevation can be obtained to within about a kilometer

under favorable retrieval conditions, e.g., when there is sufficient AOD (Satheesh et al. 2009). The UV-absorption method also makes it possible to detect aerosols when they reside over cloud, and can take advantage of the broad-swath, once-daily global coverage of the TOMS and OMI instruments (Torres et al. 2007). Because the radiative impact of absorbing species such as wildfire smoke and black carbon is enhanced when the aerosols reside above highly reflective clouds (e.g., Zarzycki and Bond 2010; Loeb and Su 2010), the ability to map these situations can make an important contribution toward reducing DARF uncertainty.

Another passive radiance technique, often called "split-window," is based on measuring top-of-atmosphere radiance differences between two channels in the infrared spectral region, usually at 11 and 12 micrometers. This approach is commonly used to obtain the elevation of condensate clouds, and has been applied to constraining the heights of fairly optically thick volcanic ash plumes, dominated by coarse-mode particles, with AVHRR as well as SEVIRI data (Prata 1989; Pavolonis et al. 2006). The vertical atmospheric weighting functions for the split-window channels typically sample within and sometimes below aerosol plumes, depending on plume characteristics, creating some ambiguity in the result.

From stereo imaging, the heights of clouds and aerosol plumes can also be derived geometrically (Moroney et al. 2002; Muller et al. 2002). This technique is not sensitive to radiometric calibration accuracy, but is effective only near aerosol sources, where plumes exhibit sufficient spatial contrast to be matched in multiple angular views; the resulting maps capture the injection heights of wildfire smoke, desert dust, and volcanic emission plumes (Kahn et al. 2007; Scollo et al. 2010; Val Martin et al. 2010). In situations where the contrast elements seen from space come from different vertical locations within the plume, a histogram loosely representing the aerosol vertical distribution is obtained. As such, the stereo-derived and lidar aerosol elevation products tend to be complementary, one providing sufficient coverage to map aerosol injection height and near-source plume behavior, and the other having the sensitivity to characterize extended aerosol layers downwind (Kahn et al. 2008), a combination that offers powerful constraints on aerosol transport models.

Satellites also retrieve surface albedo and bidirectional reflectance distribution function (BRDF), the viewing- and solar-geometry dependent surface reflection property needed to specify the lower boundary condition for DARF calculations. Several of the aerosol retrieval approaches self-consistently derive surface reflectance parameters (e.g., Martonchik et al. 2009; Lyapustin and Wang 2009; Pinty et al. 2000; Govaerts et al. 2010), and the standard MODIS BRDF product (Schaaf et al. 2002) is widely used. Limited validation data are available for these products (e.g., Román et al. 2009), but it is beyond the scope of the current paper to review this subject in greater depth.

3 A Way Forward

Enormous advances have been made in space-based aerosol remote sensing. Yet some measurements needed to constrain DARF globally at the required level-of-accuracy elude these techniques. AOD sensitivity seems to be at least within reach, if not yet within grasp, but particle size is only loosely constrained, and SSA even less so, especially when multiple aerosol components are present in the atmospheric column. Detailed SSA, particle shape, indices of refraction, and compositional information needed to identify the anthropogenic fraction are obtained primarily by collecting samples of the particles

themselves, in situ. Further, the observations from those space-based instruments yielding the most particle-microphysical-property detail fly in polar orbit, providing once-daily global snapshots at best, and cannot retrieve under clouds and in other regions where algorithmic issues arise, such as over most mountainous, snow, and ice-covered surfaces, so significant gaps remain in spatial and diurnal coverage.

Surface stations are deployed in places to sample near-surface aerosols such as pollution particles in urban settings. Such stations are often equipped to measure particle size and mass, as well as to collect samples for chemical analysis. Intensive field campaigns can provide more complete atmospheric characterization, at least on a regional basis; these involve aircraft, satellites, and ground stations making coordinated observations, often with the help of predictions from aerosol transport models.

A next-generation satellite instrument suite will likely encompass all the capabilities of previous efforts, including the wide-swath, sub-kilometer-pixel-resolution imaging of a MODIS-like instrument, with multiple viewing angles, spectral channels from the near-UV to the infrared and polarized bands, along with advanced lidar systems. High-precision multi-angular, multispectral polarization measurements offer the promise of adding important aerosol-type discrimination ability to a space-based remote-sensing instrument, retrieving in the future at least one additional moment in the particle size distribution and tighter constraints on real part of the refractive index, and offering greater flexibility in performing aerosol retrievals (Mishchenko and Travis 1997; Hasekamp and Landgraf 2007). Yet, it is not clear that the aerosol microphysical property information retrieved from even next-generation space-based remote sensing alone can provide enough quantitative detail to achieve the required improvement in global aerosol direct radiative forcing estimates.

One important simplifying factor for global-scale aerosol studies is that aerosols tend to be transported long distances in relatively thin atmospheric layers, so near-source plume height mapping combined with downwind lidar curtains offer significant constraints on vertical distribution. Another simplifying factor is that for most aerosol sources and specified seasons, emitted and evolved particle microphysical and chemical properties tend to be repeatable, even if the aerosol amounts vary considerably from day-to-day and year-to-year. This means it is at least feasible for an airborne observing program, aimed at routinely measuring particle properties in situ, to capture probability distribution functions (PDFs) of particle size, spectral absorption and scattering, shape, chemical composition, hygroscopic properties, and mass extinction efficiency, thereby characterizing the major aerosol-air-mass types in enough detail to adequately address the global aerosol direct radiative forcing problem.

This approach amounts to: (1) using satellite data to provide spatially extensive snapshots of AOD and aerosol type, as well as vertical distribution, with the coverage and at the level-of-detail possible, (2) relying on the accuracy of direct, suborbital measurements, targeted with the help of satellite aerosol-air-mass-type mapping, to assign detailed particle microphysical properties to the major aerosol-air-mass types, and (3) depending upon models, constrained by the aggregate of observational data, to calculate the regional and global radiation fields and material fluxes with adequate space–time resolution to produce the best result we can achieve.

These points are illustrated in Fig. 2. Here, satellites provide global maps of AOD and aerosol air-mass type, along with vertical distribution. Suborbital platforms perform the traditional role of validating and helping refine space-based remote-sensing retrieval algorithms, as well as providing detail unobtainable from space. Satellites also offer regional context, needed to target and appropriately interpret the in situ aerosol-air-mass-
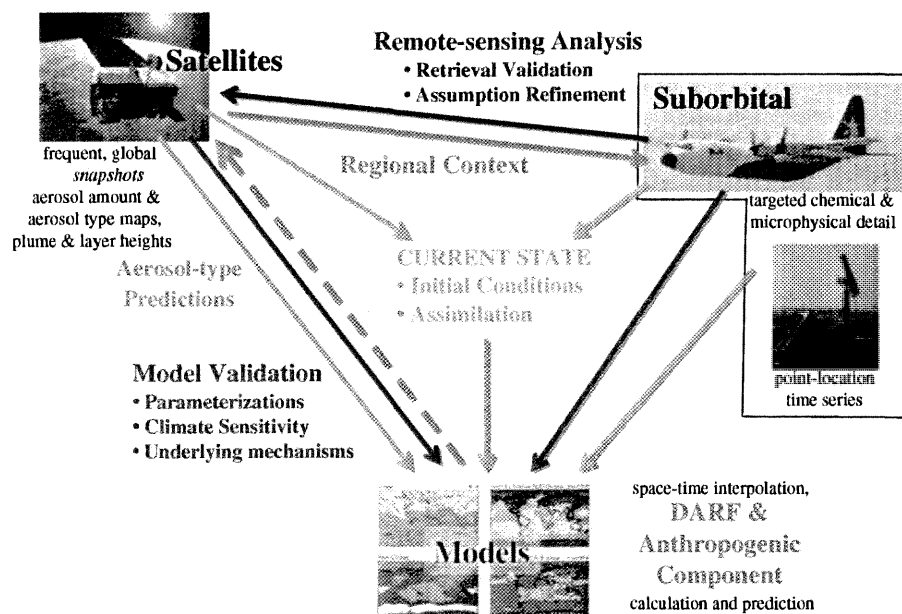
Fig. 2 Schematic representation of the relationships between satellite and suborbital measurements and models for constraining direct aerosol radiative forcing

type measurements. Taken together, these observations are used to constrain (green arrows) and validate (blue arrows) models that can calculate DARF and its anthropogenic component. The dashed pink arrow suggests the possibility of using aerosol transport model simulations to help constrain the choice of aerosol type within satellite retrieval algorithms, in situations where aerosol-type information in the satellite radiance measurements is limited.

Much work remains to reach this goal. Aerosol-type mapping from space-based remote sensing must be improved, in part by refining current retrieval algorithms, by combining data from multiple sources, and eventually by flying a next-generation instrument suite. Adequate in situ sampling of aerosol microphysical property PDFs for the major aerosol-air-mass types is needed as well. This would probably require developing and deploying a compact, low-weight instrument package that can be flown routinely and economically on a single, relatively small aircraft at least several times per week, making the requisite measurements. [A program of this type, though with somewhat different objectives, has already been successfully demonstrated (Andrews et al. 2004).] Finally, better ways of constraining aerosol transport models with the aggregate of measurements are also needed, taking account of spotty observational coverage and varying information content when establishing model result uncertainties. Yet, the goal of adequately constraining DARF is achievable, provided the aerosol measurement and modeling communities can obtain the resources, and retain the inclination, to put all the pieces together.

comments on an early version of the manuscript. The work of R. Kahn is supported in part by NASA's Climate and Radiation Research and Analysis Program, under H. Maring, NASA's Atmospheric Composition Program, and the EOS-MISR project.

References

Ackerman SA, Strabala KI, Menzel WP, Frey RA, Moeller CC, Gumley LE (1998) Discriminating clear sky from clouds with MODIS. J Geophys Res 103:32141–32157

Anderson TL, Charlson RJ, Schwartz SE, Knutti R, Bucher O, Rodhe H, Heintzenberg J (2003) Climate forcing by aerosols—a hazy picture. Science 300:1103–1104

Andreae MO, Jones CD, Cox PM (2005) Strong present-day aerosol cooling implies a hot future. Nature 435:1187–1190. doi:10.1038/nature03671

Andrews E, Sheridan PJ, Ogren JA, Ferrare R (2004) In situ aerosol profiles over the Southern Great Plains cloud and radiation test bed site: 1. Aerosol optical properties. J Geophys Res 109:D06208. doi:10.1029/2003JD004025

Bellouin N, Jones A, Haywood J, Christopher SA (2008) Updated estimate of aerosol direct radiative forcing from satellite observations and comparison against the Hadley Centre climate model. J Geophys Res 113:D10205

Cattrall C, Reagan J, Thome K, Dubovik O (2005) Variability of aerosol and spectral lidar and backscatter and extinction ratios of key aerosol types derived from selected Aerosol Robotic Network locations. J Geophys Res 110:D10S11. doi:10.1029/2004JD005124

Chen W-T, Kahn R, Nelson D, Yau K, Seinfeld J (2008) Sensitivity of multi-angle imaging to optical and microphysical properties of biomass burning aerosols. J Geophys Res 113:D10203. doi:10.1029/2007JD009414

Chin M, Kahn R, Schwartz S (eds) (2009) CCSP (U.S. Climate Change Science Program) synthesis and assessment product 2.3. Atmospheric aerosol properties and climate impacts, p 116

de Graaf M, Stammes P, Torres O, Koelemeijer RBA (2005) Absorbing aerosol index: sensitivity analysis, application to GOME and comparison with TOMS. J Geophys Res 110:D01201. doi:10.1029/2004JD005178

de Leeuw G, Kinne S, Leon JF, Pelon J, Rosenfeld D, Schaap M, Veefkind PJ, Veihelmann B, Winker DM, von Hoyningen-Huene W (2011) Retrieval of aerosol properties. In: Burrows JP, Platt U, Borrell P (eds) The remote sensing of tropospheric composition from space. Springer, Berlin, pp 359–414. doi:10.1007/978-3-642-14791-3

Deschamps PY, Bréon F-M, Leroy M, Podaire A, Bricaud A, Buriez J-C, Sèze G (1994) The POLDER mission: instrument characteristics and scientific objectives. IEEE Trans Geosci Remote Sens 32:3598–3615

Deuzé JL, Bréon FM, Devaux C, Goloub P, Herman M, Lafrance B, Maignan F, Marchand A, Nadal F, Perry G, Tanré D (2001) Remote sensing of aerosols over land surfaces from POLDER-ADEOS-1 polarized measurements. J Geophys Res 106:4913–4926

Di Girolamo L, Wilson MJ (2003) A first look at band-differenced angular signatures for cloud detection from MISR. IEEE Trans Geosci Remote Sens 41:1730–1734

Diner DJ, Beckert JC, Reilly TH, Bruegge CJ, Conel JE, Kahn R, Martonchik JV, Ackerman TP, Davies R, Gerstl SAW, Gordon HR, Muller J-P, Myneni R, Sellers RJ, Pinty B, Verstraete MM (1998) Multiangle imaging spectroradiometer (MISR) instrument description and experiment overview. IEEE Trans Geosci Remote Sens 36:1072–1087

Dubovik O, King MD (2000). A flexible inversion algorithm for retrieval of aerosol optical properties from Sun and sky radiance measurements. J Geophys Res 105(D16):20673–20696

Dubovik O, Holben BN, Eck TF, Smirnov A, Kaufman YJ, King MD, Tanré D, Slutsker I (2002) Variability of absorption and optical properties of key aerosol types observed in worldwide locations. J Atmos Sci 59:590–608

Dubovik O et al (2006) Application of spheroid models to account for aerosol particle nonsphericity in remote sensing of desert dust. J Geophys Res 111:D11208. doi:10.1029/2005JD006619

Eck TF, Holben BN, Reid JS, Dubovik O, Smirnov A, O'Neill NT, Slutsker I, Kinne S (1999) Wavelength dependence of the optical depth of biomass burning, urban, and desert dust aerosols. J Geophys Res 104:31333–31349

Eck TF et al (2008) Spatial and temporal variability of column-integrated aerosol optical properties in the southern Arabian Gulf and United Arab Emirates in summer. J Geophys Res 113:D01204. doi:10.1029/2007JD008944

Eck TF et al (2010) Climatological aspects of the optical properties of fine/coarse mode aerosol mixtures. J Geophys Res 115:D19205. doi:10.1029/2010JD014002

Flowers EC, McCormick RA, Kurfis KR (1969) Atmospheric turbidity over the United States, 1961–1966. J Appl Meteorol 8:955–962

Gao B, Kaufman YJ, Tanre D, Li R (2002) Distinguishing tropospheric aerosols from thin cirrus clouds for improved aerosol retrievals using the ratio of 1.38 μm and 1.24 μm channels. Geophys Res Lett 29. doi:10.1029/2002GL015475

Giglio L, Csiszar I, Justice CO (2006) Global distribution and seasonality of active fires as observed with the Terra and Aqua Moderate Resolution Imaging Spectroradiometer (MODIS) sensors. J Geophys Res 111. doi:10.1029/2005JG000142

Govaerts YM, Wagner SC, Lattanzio A, Watts P (2010) Joint retrieval of surface reflectance and aerosol optical depth from MSG/SEVIRI observations with an optimal estimation approach: 1. Theory. J Geophys Res 115:D02203. doi:10.1029/2009JD011779

Hasekamp OP, Landgraf J (2007) Retrieval of aerosol properties over land surfaces: capabilities of multiple-viewing-angle intensity and polarization measurements. Appl Opt 46:3332–3344

Haywood J, Schulz M (2007) Causes of the reduction in uncertainty in the anthropogenic radiative forcing of climate between IPCC (2001) and IPCC (2007). Geophys Res Lett 34:L20701. doi:10.1029/2007GL030749

Herman JR, Bhartia PK, Torres O, Hsu C, Seftor C, Celarier E (1997) Global distribution of UV-absorbing aerosols from Nimbus-7/TOMS data. J Geophys Res 102:16911–16922

Herman M, Deuzé J-L, Marchand A, Roger B, Lallart P (2005) Aerosol remote sensing from POLDER/ADEOS over the ocean: Improved retrieval using nonspherical particle model. J Geophys Res 110. doi:10.1029/2004JD004798

Holben BN et al (1998) AERONET—a federated instrument network and data archive for aerosol characterization. Remote Sens Environ 66:1–16

Holzer-Popp T, Schroedter-Homscheidt M, Breitkreuz MH, Klüser L, Martynenko D (2008) Improvements of synergetic aerosol retrieval for ENVISAT. Atmos Chem Phys 8:7651–7672

Hsu N, Tsay S, King M, Herman J (2004) Aerosol properties over bright-reflecting source regions. IEEE Trans Geosci Remote Sens 42:557–569

Hsu NC, Tsay SC, King MD, Herman JR (2006) Deep Blue retrievals of Asian aerosol properties during ACE-Asia. IEEE Trans Geosci Remote Sens 44:3180–3195

Husar RB, Prospero JM, Stowe LL (1997) Characterization of troposhperic aerosols over the oceans with the NOAA advanced very high resolution radiometer optical thickness operational product. J Geophys Res 102:16889–16909

Ichoku C, Giglio L, Wooster MJ, Remer LA (2008) Global characterization of biomass-burning patterns using satellite measurements of Fire Radiative Energy. Remote Sens Environ 112:2950–2962

Ignatov A, Sapper J, Cox S, Laszlo I, Nalli NR, Kidwell KB (2004) Operational aerosol observations (AEROBS) from AVHRR/3 on board NOAA-KLM satellites, J. Atmos Oceanic Technol 21:3–26. doi:10.1175/1520-0426(2004)021

IPCC (Intergovernmental Panel on Climate Change) (2001) Radiative forcing of climate change, in Climate Change 2001. Cambridge University Press, New York

IPCC (Inter-governmental Panel on Climate Change) (2007) The physical science basis. In: Solomon S, Qin D, Manning H, Chen Z, Marquis M, Averyt K, Tignor M, Miller H (eds) Contribution of working group I to the fourth assessment report of the intergovernmental panel on climate change. Cambridge University press

Kacenelenbogen M, Vaughan MA, Redemann J, Hoff RM, Rogers RR, Ferrare RA, Russell PB, Hostetler CA, Hair JW, Holben BN (2011) An accuracy assessment on fthe CALIOP/CALIPSO version 2/version 3 daytime aerosol extinction product based on a detailed multi-sensor, multi-platform case study. Atmos Chem Phys 11:3981–4000

Kahn R, Banerjee P, McDonald D (2001) The sensitivity of multiangle imaging to natural mixtures of aerosols over ocean. J Geophys Res 106:18219–18238

Kahn RA, Li W-H, Moroney C, Diner DJ, Martonchik JV, Fishbein E (2007) Aerosol source plume physical characteristics from space-based multiangle imaging. J Geophys Res 112:D11205. doi:10.1029/2006JD007647

Kahn RA, Chen Y, Nelson DL, Leung F-Y, Li Q, Diner DJ, Logan JA (2008) Wildfire smoke injection heights: two perspectives from space. Geophys Res Lett 35:L04809. doi:10.1029/2007GL032165

Kahn R, Petzold A, Wendisch M, Bierwirth E, Dinter T, Esselborn M, Fiebig M, Heese B, Knippertz P, Muller D, Schladitz A, von Hoyningen-Huene W (2009) Desert dust aerosol air mass mapping in the Western Sahara, using particle properties derived from space-based multi-angle imaging. Tellus 61B:239–251. doi:10.1111/j.1600-0889.2008.00398.x

Kahn RA, Gaitley BJ, Garay MJ, Diner DJ, Eck T, Smirnov A, Holben BN (2010) Multiangle Imaging SpectroRadiometer global aerosol product assessment by comparison with the Aerosol Robotic Network. J Geophys Res 115:D23209. doi:10.1029/2010JD014601

Kahn RA, Garay MJ, Nelson DL, Levy RC, Bull MA, Diner DJ, Martonchik JV, Hansen EG, Remer LA, Tanré D (2011) Response to "Toward unified satellite climatology of aerosol properties. 3. MODIS versus MISR versus AERONET." J Quant Spectro Rad Transf 112:901–909. doi:10.1016/j.jqsrt.2009.11.003

Kalashnikova OV, Kahn R (2006) Ability of multiangle remote sensing observations to identify and distinguish mineral dust types: part 2. Sensitivity over dark water. J Geophys Res 111:D11207. doi:10.1029/2005JD006756

Kaufman YJ, Tanré D, Remer LA, Vermote EF, Chu DA, Holben BN (1997) Operations remote sensing of tropospheric aerosol over land from EOS moderate resolution imaging spectroradiometer. J Geophys Res 102:17051–17067

Kaufman YJ, Remer L, Tanré D, Li R, Kleidman R, Mattoo S et al (2005a) A critical examination of the residual cloud contamination and diurnal sampling effects on MODIS estimates of aerosol over ocean. IEEE Trans Geosci Remote Sens 43:2886–2897

Kaufman YJ, Boucher O, Tanré D, Chin M, Remer LA, Takemura T (2005b) Aerosol anthropogenic component estimated from satellite data. Geophys Res Lett 32. doi:10.1029/2005/GL023125

Kiehl JT (2007) Twentieth century climate model response and climate sensitivity. Geophys Res Lett 34. doi:10.1029/2007/GL031383

Kim D, Ramanathan V (2008) Solar radiation budget and radiative forcing due to aerosols and clouds. J Geophys Res 113. doi:10.1029/2007JD008434

Kim D-H, Sohn B-J, Nakajima T, Takamura T, Takemura T, Choi B-C, Yoon S-C (2004) Aerosol optical properties over East Asia determined from ground-based sky radiation measurements. J Geophys Res 109:D02209. doi:10.1029/2003JD003387

King MD, Byrne DM, Herman BM, Reagan JA (1978) Aerosol size distributions obtained by inversion of spectral optical depth measurements. J Atmosph Sci 35:2153–2167

Kinne S, Schulz M, Textor C et al (2006) An AeroCom initial assessment—optical properties in aerosol component modules of global models. Atmos Chem Phys 6:1815–1834

Knapp KR (2002) Quantification of aerosol signal in the GOES 8 visible imagery over the United States. J Geophys Res 107. doi:10.1029/2001JD002001

Knapp KR, Frouin R, Kondradunta S, Prados A (2007) Toward aerosol optical depth retrievals over land from GOES visible radiances: determining surface reflectance. Int J Remote Sens 26:4097–4116

Kokhanovsky A, de Leeuw G (eds) (2009) Satellite aerosol remote sensing over land. Springer, Berlin, p 388

Laszlo I, Ciren P, Liu H, Kondragunta S, Tarpley JD, Glodberg MD (2008) Remote sensing of aerosol and radiation from geostationary satellites. Adv Space Res 41:1882–1893

Levy RC, Remer LA, Dubovik O (2007) Global aerosol optical properties and application to Moderate Resolution Imaging Spectroradiometer aerosol retrieval over land. J Geophys Res 112:D13210. doi:10.1029/2006JD007815

Levy RC, Remer LA, Kleidman RG, Mattoo S, Ichoku C, Kahn R, Eck TF (2010) Global evaluation of the Collection 5 MODIS dark-target aerosol products over land. Atmos Chem Phys 10:10399–10420. doi:10.5194/acp-10-10399-2010

Loeb NG, Manalo-Smith N (2005) Top-of-atmosphere direct radiative effect of aerosol over global oceans from merged CERES and MODIS observations. J Climate 18:3506–3526

Loeb NG, Su W (2010) Direct aerosol radiative forcing uncertainty based on a radiative perturbation analysis. J Climate 23:5288–5293

Lyapustin A, Wang Y (2009) The time series technique of aerosol retrievals over land from MODIS. In: Kokhanovsky A, de Leeuw G (eds) Satellite aerosol remote sensing over land. Springer, Berlin, pp 69–99

Lyapustin A, Wang Y, Laszlo I, Kahn R, Korkin S, Remer L, Levy R, Reid JS (2011) Multiangle implementation of atmospheric correction (MAIAC): 2. Aerosol algorithm. J Geophys Res 116:D03211. doi:10.1029/2010JD014986

Marshak A, Wen G, Coakley JA, Remer LA, Loeb NG, Cahalan RF (2008) A simple model for the cloud adjacency effect and the apparent bluing of aerosols near clouds. J Geophys Res 113. doi:10.1029/2007JD009196

Martins JV, Tanre D, Remer L, Kaufman Y, Mattoo S, Levy R (2002) MODIS cloud screening for remote sensing of aerosol over oceans using spatial variability. Geophys Res Lett 29. doi:10.1029/2001GL013252

Martonchik JV, Diner DJ, Crean KA, Bull MA (2002) Regional aerosol retrieval results from MISR. IEEE Trans Geosci Remote Sens 40:1520–1531

Martonchik JV, Kahn RA, Diner DJ (2009) Retrieval of aerosol properties over land using MISR observations. In: Kokhanovsky A, de Leeuw G (eds) Satellite aerosol remote sensing over land. Springer, Berlin, pp 267–293

McComiskey A, Schwartz SE, Schmid B, Guan H, Lewis ER, Ricchiazzi P, Ogren JA (2008) Direct aerosol forcing: calculation from observables and sensitivities to inputs. J Geophys Res 113:D09202. doi:10.1029/2007JD009170

Mishchenko MI, Geogdzhayev IV (2007) Satellite remote sensing reveals regional tropospheric aerosol trends. Opt Exp 15:7423–7438

Mishchenko MI, Travis LD (1997) Satellite retrieval of aerosol properties over the ocean using polarization as well as intensity of reflected sunlight. J Geophys Res 102:16989–17012

Mishchenko MI, Geogdzhayev IV, Cairns B, Rossow WB, Lacis AA (1999) Aerosol retrievals over the ocean by use of channels 1 and 2 AVHRR data: sensitivity analysis and preliminary results. Appl Opt 38:7325–7341

Moroney C, Davies R, Muller J-P (2002) Operational retrieval of cloud-top heights using MISR data. IEEE Trans Geosci Remote Sens 40:1532–1540

Muller J-P, Mandanayake A, Moroney C, Davies R, Diner DJ, Paradise S (2002) Operational retrieval of cloud-top heights using MISR data. IEEE Trans Geosci Remote Sens 40:1532–1546

Myhre G et al (2009) Modelled radiative forcing of the direct aerosol effect with multi-observation evaluation. Atmos Chem Phys 9:1365–1392

North PRJ (2002) Estimation of aerosol opacity and land surface bidirectional reflectance from ATSR-2 dual-angle imagery: operational method and validation. J Geophys Res 107. doi:10.1029/2000JD000207

Omar AH, Winker DM, Kittaka C et al (2009) The CALIPSO automated aerosol classification and lidar ratio selection algorithm. J Atm Ocean Tech 26:1994–2014

Pavolonis MJ, Feltz WF, Heidinger AK, Gallina GM (2006) A daytime complement to the reverse absorption technique for improved automated detection of volcanic ash. J Atmos Oceanic Tech 23:1422–1444

Pierce JR, Kahn RA, Davis MR, Comstock JM (2010) Detecting thin cirrus in multiangle imaging spectroradiometer aerosol retrievals. J Geophys Res 115:D08201. doi:10.1029/2009JD013019

Pinty B, Roveda F, Verstraete MM, Gobron N, Govaerts Y, Martonchik JV, Diner DJ, Kahn RA (2000) Surface albedo retrieval from Meteosat: 2. Applications J Geophys Res 105:18113–18134

Popp C, Hauser A, Foppa N, Wunderle S (2007) Remote sensing of aerosol optical depth over central Europe from MSG-SEVIRI data and accuracy assessment with ground-based AERONET measurements. J Geophys Res 112:D24S11. doi:10.1029/2007JD008423

Prata AJ (1989) Observations of volcanic ash clouds in the 10–12 micrometer window using AVHRR/2 data. Int J Remote Sens 10:751–761

Prospero JM, Ginoux P, Torres O, Nicholson SE, Gill TE (2002) Environmental characterization of global sources of atmospheric soil dust identified with the Nimbus 7 Total Ozone Mapping Spectrometer (TOMS) absorbing aerosol product. Rev Geophys 40. doi:10.1029/2000RG000095

Quaas J, Boucher O, Bellouin N, Kinne S (2008) Satellite-based estimate of the direct and indirect aerosol climate forcing. J Geophys Res 113. doi:10.1029/2007JD008962

Remer LA, Kaufman YJ, Tanre D, Mattoo S, Chu DA, Martins JV, Li R–R, Ichoku C, Levy RC, Kleidman RG, Eck TF, Vermote E, Holben BN (2005) The MODIS aerosol algorithm, products, and validation. J Atmos Sci 62:947–973

Remer LA, Kleidman RG, Levy RC, Kaufman YJ, Tanre D, Mattoo S, Martins JV, Ichoku C, Koren I, Yu H, Holben BN (2008) Global aerosol climatology from the MODIS satellite sensors. J Geophys Res113. doi:10.1029/2007JD009661

Román MO, Schaaf CB, Yang X, Woodcock CE, Strahler AH, Braswell RH et al (2009) The MODIS (Collection V005) BRDF/albedo product: assessment of spatial representativeness over forested landscapes. Remote Sens Environ 113:2476–2498. doi:10.1016/j.rse.2009.07.009

Satheesh SK, Torres O, Remer LA, Babu SS, Vinoj V, Eck TF, Kleidman RG, Holben BN (2009) Improved assessment of aerosol absorption using OMI-MODIS joint retrieval. J Geophys Res 114. doi:10.1029/2008JD011024

Schaaf CB et al (2002) First operational BRDF, Albedo and Nadir reflectance products from MODIS. Remote Sens Environ 83:135–148

Schuster GL, Dubovik O, Holben BN (2006) Angstrom exponent and bimodal aerosol size distributions. J Geophys Res 111:D07207. doi:10.1029/2005JD006328

Schwartz SE, Charlson RJ, Kahn RA, Ogren JA, Rodhe H (2010) Why hasn't Earth warmed as much as expected? J Clim 23:2453–2464

Scollo S, Folch A, Coltelli M, Realmuto VJ (2010) Three-dimensional volcanic aerosol dispersal: a comparison between Multiangle Imaging Spectroradiometer (MISR) data and numerical simulations. J Geophys Res 115:D24210. doi:10.1029/2009JD013162

Smirnov A, Holben BN, Slutsker I, Giles DM, McClain CR, Eck TF, Sakerin SM, Macke A, Croot P, Zibordi G, Quinn PK, Sciare J, Kinne S, Harvey M, Smyth TJ, Pikety S, Zielinski T, Proshutinsky A, Goes JI, Nelson NB, Larouche P, Radionov VF, Goloub P, Krishnamoorthy K, Matarrese R, Robertson EJ, Jourdin F (2009) Maritime aerosol network as a component of aerosol robotic network. J Geophys Res 114:D06204. doi:10.1029/2008JD011257

Stowe LL, Ignatov AM, Singh RR (1997) Development, validation, and potential enhancements to the second-generation operational aerosol product at the National Environmental Satellite, Data, and Information Service of the National Oceanic and Atmospheric Administration. J Geophys Res 102:16923–16934

Stowe LL, Wellemeyer CG, Eck TF, Yeh HYM, Nimbus-7 cloud processing team (1998) Nimbus-7 global cloud climatology. Part I: Algorithms and validation. J Clim 5:445–470

Tackett JL, Di Girolamo L (2009) Enhanced aerosol backscatter adjacent to torpical trade wind clouds revealed by satellite-based lidar. Geophys Res Lett 36. doi:10.1029/2009GL039264

Tanré D, Kaufman YJ, Herman M, Mattoo S (1997) Remote sensing of aerosol properties over oceans using the MODIS/EOS spectral radiances. J Geophys Res 102:16971–16988

Torres O, Bhartia PK, Herman JR, Ahmad Z, Gleason J (1998) Derivation of aerosol properties from satellite measurements of backscattered ultraviolet radiation: theoretical basis. J Geophys Res 103:17099–17110

Torres O, Bhartia PK, Herman JR, Syniuk A, Ginoux P, Holben B (2002) A long-term record of aerosol optical depth from TOMS observations and comparison to AERONET measurements. J Atmos Sci 59:398–413

Torres O, Tanskanen A, Veihelmann B, Ahn C, Braak R, Bhartia PK, Veefkind P, Levelt P (2007) Aerosols and surface UV products from Ozone Monitoring Instrument observations: an overview. J Geophys Res 112:D24S47. doi:10.1029/2007JD008809

Twohy CH, Coakley JA, Tahnk WR (2009) Effect of changes in relative humidity on aerosol scattering near clouds. J Geophys Res 114:D05205. doi:10.1029/2008JD010991

Val Martin M, Logan JA, Kahn R, Leung F-Y, Nelson D, Diner D (2010) Fire smoke injection heights over North America constrained from the Terra Multi-angle Imaging SpectroRadiometer. Atm Chem Phys 10:1491–1510

Várnai T, Marshak A (2011) Global CALIPSO observations of aerosol changes near clouds. IEEE Geosci Remote Sens Lett 8:19–23

Veefkind JP, de Leeuw G, Durkee PA (1998) Retrieval of aerosol optical depth over land using two-angle view satellite radiometry during TARFOX. Geophys Res Lett 25:3135–3138

Veefkind JP, de Leeuw G, Stammes P, Koelemeijer RBA (2000) Regional distribution of aerosol over land, derived from ATSR-2 and GOME. Remote Sens Environ 74:377–386

von Hoyningen-Huene W, Kokhanovsky AA, Wuttke MW, Buchwitz M, Noel S, Gerilowski K, Burrows JP, Latter B, Siddans R, Kerridge BJ (2007) Validation of SCIAMACHY top-of-atmosphere reflectance for aerosol remote sensing using MERIS L1 data. Atmos Chem Phys 7:97–106

Wagner SC, Govaerts YM, Lattanzio A (2010) Joint retrieval of surface reflectance and aerosol optical depth from MSG/SEVIRI observations with an optimal estimation approach: 2. Implementation and evaluation. J Geophys Res 115:D02204. doi:10.1029/2009JD011780

Waquet F, Léon J-F, Cairns B, Goloub P, Deuzé J-L, Auriol F (2009) Analysis of the spectral and angular response of the vegetated surface polarization for the purpose of aerosol remost esesing over land. Appl Opt 48:1228–1236

Whitby KT (1978) The physical characteristics of sulfur aerosols. Atmos Environ 12:135–159

Winker DM, Vaughan MA, Omar A, Hu Y, Powell KA, Liu Z, Hunt WH, Young SA (2009) Overview of the CALIPSO mission and CALIOP data processing algorithms. J Atmos Ocean Tech 26:2310–2323

Yu H, Kaufman YJ, Chin M, Feingold G, Remer LA, Anderson TL, Balkanski Y, Bellouin N, Boucher O, Christopher S, DeCola P, Kahn R, Koch D, Loeb N, Reddy MS, Schulz M, Takemura T, Zhou M (2006) A review of measurement-based assessment of aerosol direct radiative effect and forcing. Atmos Chem Phys 6:613–666

Yu H, Remer LA, Chin M, Bian H, Kleidman RG, Diehl T (2008) A satellite-based assessment of trans-pacific transport of pollution aerosol. J Geophys Res 113:D14S12. doi:10.1029/2007JD009349

Zarzycki CM, Bond TM (2010) How much can the vertical distribution of black carbon affect its global direct radiative forcing? Geophys Res Lett 37:L20807. doi:10.1029/2010GL044555

Zhang J, Reid JS (2006) MODIS aerosol product analysis for data assimilation: assessment of over-ocean level 2 aerosol optical thickness retrievals. J Geophys Res 111:D22207. doi:10.1029/2005JD006898

Zhang J, Reid JS (2010) A decadal regional and global trend analysis of the aerosol optical depth using a data-assimilation grade over-water MODIS and Level 2 MISR aerosol products. Atmos Chem Phys 10. doi:10.5194/acp-10-1-2010

Zhao G, Di Girolamo L (2004) A cloud fraction versus view angle technique for automatic in scene evaluation of the MISR cloud mask. J Appl Meteorol 43:860–869. doi:10.1175/1520-0450

Zhao G, Di Girolamo L, Dey S, Jones AL, Bull M (2009) Examination of direct cumulus contamination on MISR-retrieved aerosol optical depth and angstrom coefficient over ocean. Geophys Res Lett 36. doi:10.1029/2009GL038549